Slagter, S., et al., 2020, Experimental evidence supports early silica cementation of the Ediacara Biota: Geology, v. 49, https://doi.org/10.1130/G47919.1

Experimental evidence supports early silica cementation of the Ediacara Biota

Silvina Slagter[1], Lidya G. Tarhan[1], Weiduo Hao[2], Noah J. Planavsky[1], and Kurt O. Konhauser[2]

[1]*Department of Earth and Planetary Sciences, Yale University, New Haven, CT 06511, USA*

[2]*Department of Earth and Atmospheric Sciences, University of Alberta, Edmonton, AB T6G 2E3, Canada*

METHODS

Experimental Materials

Carolina Biological Supply Company (Burlington, NC, USA) product numbers:

Cinachyra alloclada (Prod. No. #162927)

Cassiopea (Prod. No. #162936)

Phymanthus crucifer (Prod. No. #162942)

Marsilea (Prod. No. #156931)

Spirulina (Prod. No. #151900)

Water and tissue sampling

Water samples (2 mL) were removed by syringe at various intervals and stored in tightly capped polyethylene containers for analysis of silica concentration. Part (0.2 ml) of each sample was separated to evaluate pH change over time using serological pipettes (Table DR1). Solution pH was measured using a Thermo Scientific™ Orion™ PerpHecT™ ROSS™ Combination pH Micro Electrode, calibrated with the pH buffers 4.0, 7.0, 10.0 before each analysis. The error associated with the pH measurement is within ±0.02 log units (2σ). Organic tissues were also sampled at the same intervals for scanning electron microscope and energy-dispersive x-ray spectroscopy (SEM-EDS) observations. Concentrations of silica were measured by the molybdate blue method with metol as the reducing agent (Mullin and Riley, 1955) at 812 nm using a UV/VIS spectrophotometer (Table DR2).

Organic tissue samples were fixed in 4% paraformaldehyde, stored at 4ºC, and then coated with 6 nm platinum for SEM-EDS analysis with a Secondary Electron (SE) detector. SEM-EDS analyses were performed at 3-10 kV with a FEI XL-30 scanning electron microscope and a Hitachi SU7000 in the Department of Earth and Planetary Sciences at Yale University. Specimen dimensions and weights are detailed in Table DR3.

Acid-base titrations

Potentiometric acid-base titrations were performed at the Department of Earth and Atmospheric Sciences at the University of Alberta. Analyses were performed for each tissue type (5 samples of each) to determine their proton reactivities. Before each titration, the pH electrode was calibrated using commercial pH buffers (Thermo Fisher Scientific; pH 4.0, 7.0, 10.0). For each titration, organic tissues were suspended in a 0.56 M NaCl solution. The suspension was then bubbled for 30 min with N_2(g) to ensure the solution was devoid of CO_2. During titrations, the experimental apparatus remained sealed and was continuously bubbled with N_2 to prevent CO_2 from entering the system. Each organic tissue sample was titrated over a pH range of 3.0 to 10.5. Initially, a small volume of 0.1 M nitric acid (HNO_3, ACS certified, Fisher Scientific) was added to bring pH to 3.0, and then 0.1 M sodium hydroxide (NaOH, ACS certified, Fisher Scientific) solution was incrementally added to bring the pH up to 10.5 (forward titration). To test the hysteresis of the samples, a backward titration was performed after each forward titration by adding acid to decrease the solution pH from 10.5 to 3.0. After the volume of acid and base were added, the corresponding pH changes were recorded at each titration step. The pH was considered stable only after the electrode achieved a reading of 12 mV/min. A blank titration, without the addition of biomass, was performed for electrolyte solutions at each of the titrations performed.

Surface complexation modeling was performed for acid-base titration results of organic tissue samples. Three types of surface functional groups (≡LH, ≡XH, ≡MH) were invoked to represent surface proton-reactive groups. The protonation behaviors of the three surface sites are described as follows:

$$\equiv L^- + H^+ \leftrightarrow \equiv LH \qquad \text{(R1)}$$

$$K_{a1} = \frac{[\equiv LH]}{[\equiv L^-] \bullet \alpha_{H^+}} \qquad \text{(eq. 1)}$$

$$\equiv X^- + H^+ \leftrightarrow \equiv XH \qquad \text{(R2)}$$

$$K_{a2} = \frac{[\equiv XH]}{[\equiv X^-] \bullet \alpha_{H^+}} \qquad \text{(eq. 2)}$$

$$\equiv M^- + H^+ \leftrightarrow \equiv MH \qquad \text{(R3)}$$

$$K_{a3} = \frac{[\equiv MH]}{[\equiv M^{-}] \bullet \alpha_{H^+}} \quad \text{(eq. 3)}$$

where square brackets denote the concentration of surface functional groups and α_{H+} the activity of protons in solution; K values derived by equations 1-3 are proton interaction constants that govern the adsorption and desorption of protons from the sample's surfaces.

A surface complexation model (SCM) was generated using the titration data and the modeling software FITEQL 4.0 (Westall, 1982) in order to calculate K_a values and ligand concentrations that best describe the excess charge data. The initial protonation stage was estimated based on Fein et al. (2005).

Table S1. pH measurements

Hour		0	1	2	18	26	48	97	117	121	141	144	148
Cassiopea	1	7.8	7	7.8	7	6.7	6.7	7.8	7.8	7.8	7.5	7.4	7.7
	2	7.8	7.7	7.7	7.8	8	7.8	7.7	7.7	7.7	7.7	7.5	7.7
	3	7.7	7.7	7.6	7.6	7.6	7.6	7.6	7.5	7.7	7.5	7.4	7.4
Cynachira	1	7.8	7.1	6.9	6.8	6.9	6.7	7.6	6.8	6.9	7.2	7.7	7.3
	2	7.8	7.8	7.8	7.8	7.8	7.8	7.8	7.8	7.8	7.8	7.8	7.2
	3	7.8	7.8	7.8	7.8	7.8	7.8	7.7	7.8	7.8	7.6	7.6	7.8
Spirulina	1	7.8	7.8	7.8	7.8	7.8	7.8	7.8	7.8	7.8	7.8	7.8	7.8
	2	7.8	7.8	7.8	7.8	7.8	7.8	7.8	7.8	7.8	7.8	7.8	7.8
	3	7.8	8	7.6	7.8	7.1	7.8	7.8	7.8	7.8	7.8	7.8	7.8
Marsilea	1	7.8	7.8	7.8	7.8	7.8	7.8	7.8	7.8	7.8	7.8	7.8	7.8
	2	7.8	7.8	7.7	7.8	7.6	7.8	7.8	7.7	7.8	7.8	7.8	7.8
	3	7.8	7.8	7.8	7.8	7.8	7.8	7.8	7.8	7.8	7.8	7.8	7.8
Phymantus	1	7.8	7.8	7.8	7.8	7.8	7.8	7.8	7.8	7.8	7.8	7.8	7.8
	2	7.8	7.8	7.8	7.8	7.7	7.8	7.8	7.8	7.8	7.8	7.8	7.8
	3	7.8	7.8	7.8	7.8	7.8	7.8	7.8	7.8	7.8	7.8	7.8	7.8
Quercus	1	7.8	7.8	7.8	7.8	7.7	7.8	7.8	7.8	7.8	7.8	7.8	7.8
	2	7.8	7.8	7.8	7.8	7.8	7.8	7.8	7.8	7.8	7.8	7.8	7.8
	3	7.8	7.8	7.8	7.8	7.8	7.8	7.8	7.8	7.8	7.8	7.8	7.8
control	1	7.8	7.8	7.8	7.8	7.8	7.8	7.8	7.8	7.8	7.8	7.7	7.8
	2	7.8	7.8	7.8	7.8	7.8	7.8	7.8	7.8	7.8	7.8	7.8	7.7
	3	7.8	7.8	7.8	7.8	7.8	7.8	7.7	7.8	7.8	7.6	7.6	7.7

Table S2: List of ingredients for silica assay*

Reagent	Concentration (g solute/500 mL ddH_2O)
Molybdate reagent	
Ammonium molybdate	4
12N Hydrochloric acid	12.0†
Reducing reagent	
Metol-sulfite	
Anhydrous sodium sulfite	6
P-methyl aminophenol sulfate	10
Oxalic acid solution	50
Sulfuric acid (50%)	250.0†

Note: The molybdate reagent, metol-sulfite, oxalic acid and sulfuric acid solutions were prepared independently in 500 mL of ddH_2O. Metol-sulfite, oxalic acid and sulfuric acid were mixed together to form the reducing agent (5:3:3, respectively, v/v/v). 2 mL of molybdate reagent and 3 mL of reducing reagent were added to 4 mL of sample before analyzing silica concentrations. Blanks and standard were prepared by the addition of 0.2 ml of artificial seawater to 3.8 ml of initial sample.
* Modified from Newman et al. (2016)
† Represents the addition of a liquid volume (in mL).

Table S3. Sample dimension, weight and time of decay

Sample		Diameter (cm)	Weight (g)	Time to complete decay (h)
Cassiopea	1	7.1	5.09	130
	2	7.2	6.21	125
	3	6.8	4.89	125
Cynachira	1	6.8	6.88	N.D*
	2	5.2	5.77	N.D*
	3	6.8	5.11	N.D*
Spirulina	1	0.5	1.023	132
	2	0.3	2.33	130
	3	0.25	0.23	123
Marsilea	1	N.D*	5.3	N.D*
	2	N.D*	8	N.D*
	3	N.D*	7.23	N.D*
Phymantus	1	1.2	4	142
	2	1.5	4.8	147
	3	2	5	150
Quercus	1	N.D*	2.3	N.D*
	2	N.D*	2.2	N.D*
	3	N.D*	2.1	N.D*

*N.D: not determined

Table S4. Summary of acid-base titration and SCM results and comparison with literature results. Site density and pKa values represent the average values of all replicates.

	Ligand class	Average pKa	Mean site concentration (mol/g)	Functional group[a]
Cassiopea	LH	4.09	8.01E-06	Carboxyl
	XH	6.41	3.69E-06	Carboxyl or phosphoryl
	MH	9.57	3.45E-05	Amino
Cynachira	LH	4.48	2.16E-04	Carboxyl
	XH	6.49	2.62E-05	Carboxyl or phosphoryl
	MH	9.59	3.18E-04	Amino
Spirulina	LH	6.37	1.33E-05	Carboxyl or phosphoryl
	XH	9.1	6.26E-04	Amino
	MH	10.39	1.06E-04	Amino
Marsilea	LH	4.22	1.39E-04	Carboxyl
	XH	6.47	3.76E-05	Carboxyl or phosphoryl
	MH	9.62	6.41E-05	Amino
Phymantus	LH	4.48	4.04E-04	Carboxyl
	XH	7.18	2.64E-05	Phosphoryl
	MH	9.64	4.57E-04	Amino
Quercus	LH	5.14	3.25E-05	Carboxyl
	XH	7.37	4.44E-05	Phosphoryl
	MH	9.4	8.53E-05	Amino
Literature results for biomass titration and SCM				
Calothrix isolated sheath[b]	LH	4.62	3.30E-05	Carboxyl
	XH	6.12-7.26	1.4-2.7E-05	Carboxyl or phosphoryl
	MH	8.06-9.15	2.3-4.1E-05	Amino
Worm mucus[c]	LH	4.89	5.20E-03	Carboxyl
	XH	6.93	3.55E-03	Phosphoryl
	MH	8.98	2.51E-03	Thiol
Worm mucus[d]	LH	4.82	5.73E-03	Carboxyl
	XH	7.08	4.67E-03	Phosphoryl
	MH	9.3	6.89E-03	Thiol or amino
Synechococcus sp. PCC 7002[e]	LH	5.07-5.42	1.17-1.51E-02	Carboxyl
	XH	6.71-7.42	5.72-6.55E-03	Phosphoryl
	MH	8.54-9.95	6.96-11.07E-03	Amino
Alginate[f]	LH	3.98	1.73E-03	Carboxyl
Diopatra parchment[g]	MH	-1.079613993	1.17E-05	Hydroxyl

[a] functional group estimation in this study is based on literature values (see Liu et al., 2015; Phoenix et al., 2002; Konhauser, 2009).
[b] results from Phoenix et al. (2002)
[c] results from Lalonde et al. (2010)

[d] results from Petrash et al. (2011a)
[e] results from Liu et al. (2015)
[f] results from Petrash et al. (2011b)
[g] results from Konhauser et al. (2020)

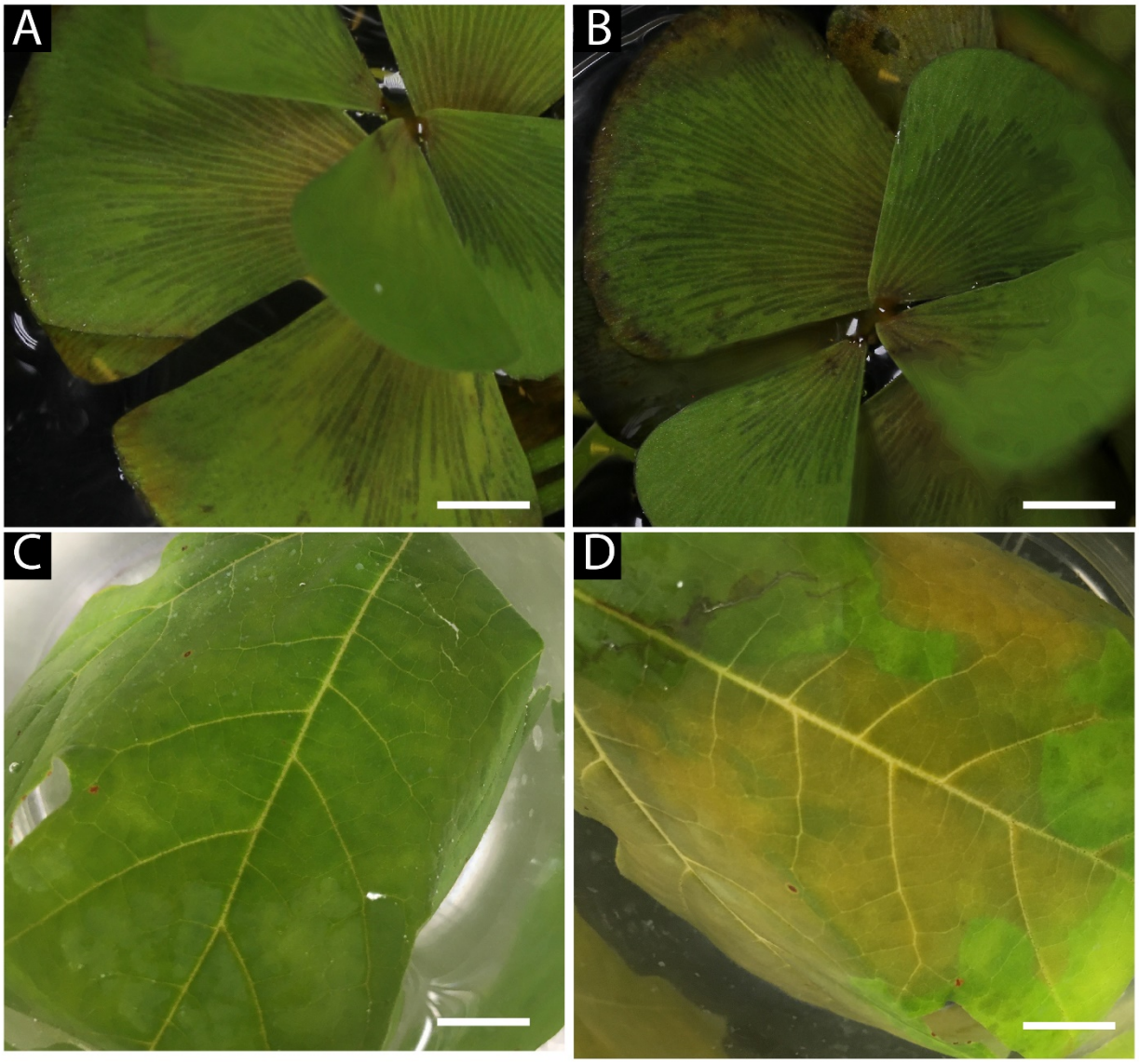

Figure S1. Images of *Marsilea* in experiments after: (A) 60 h, and (B) 120 h. Images of *Quercus* in experiments after: (C) 24 h, and (D) 96 h. Note lack of visible signs of silica precipitation. Scale bar is 2 mm.

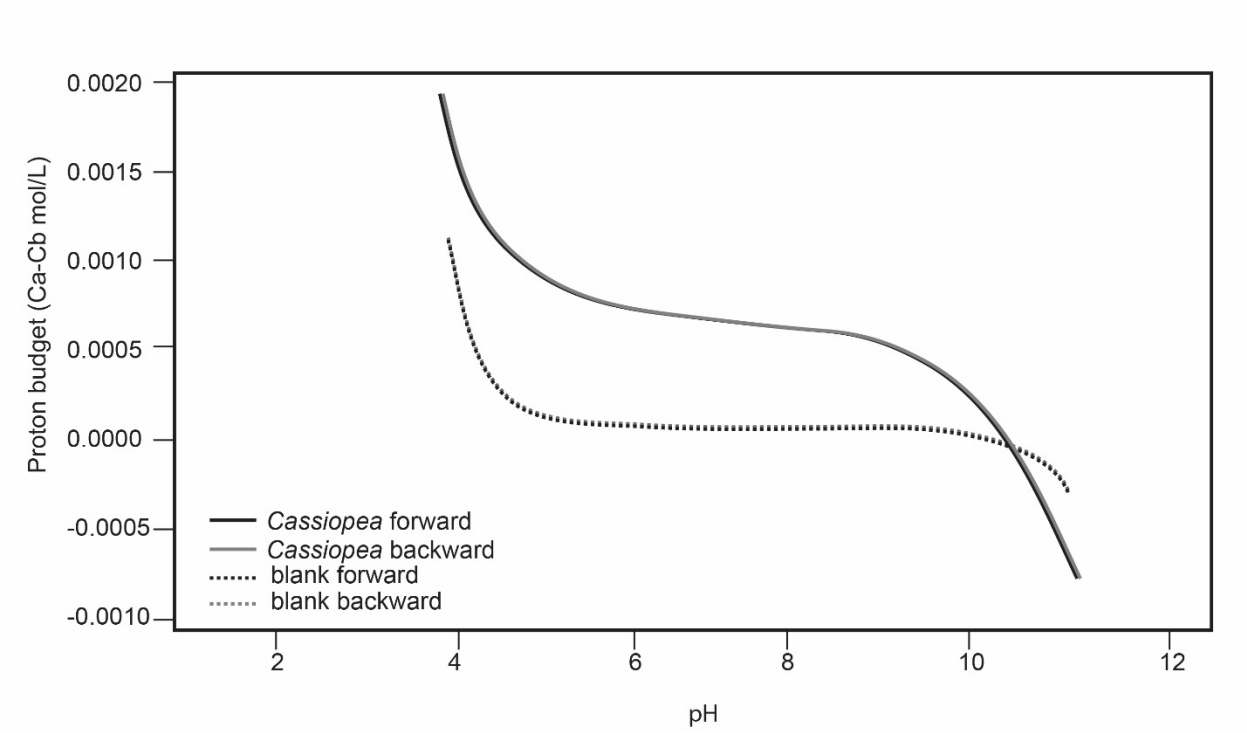

Figure S2. Acid-base titration curves for *Cassiopea*.

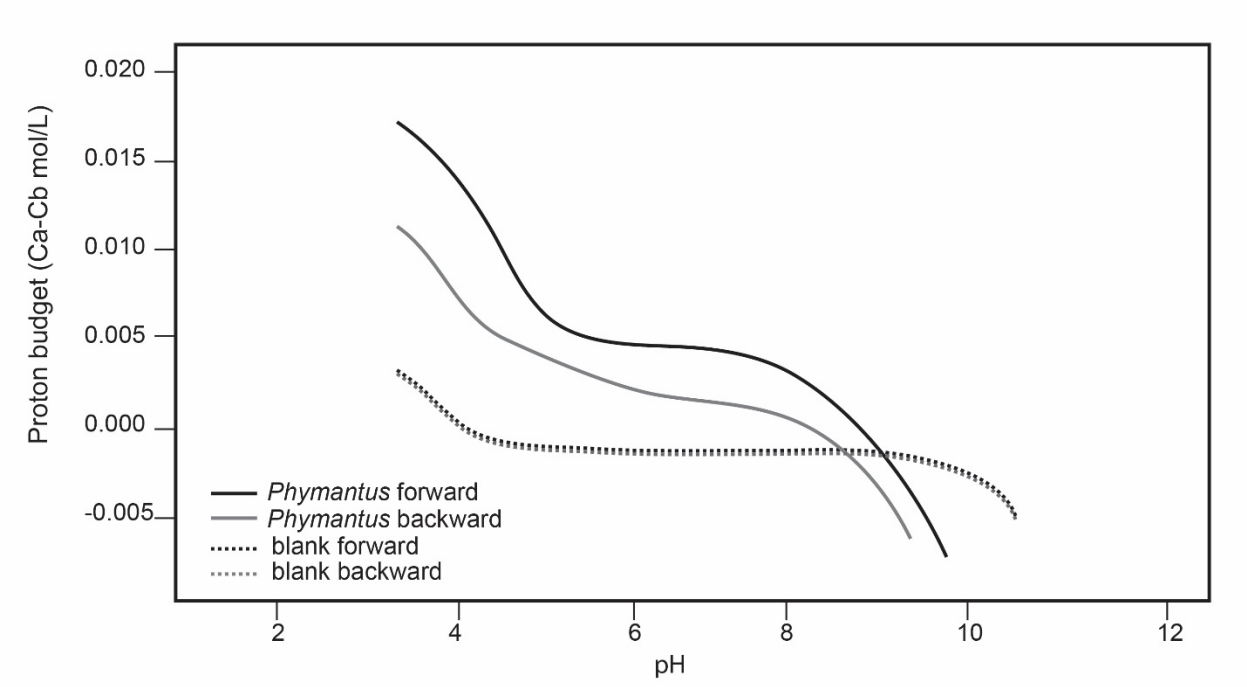

Figure S3. Acid-base titration curves for *Phymantus*.

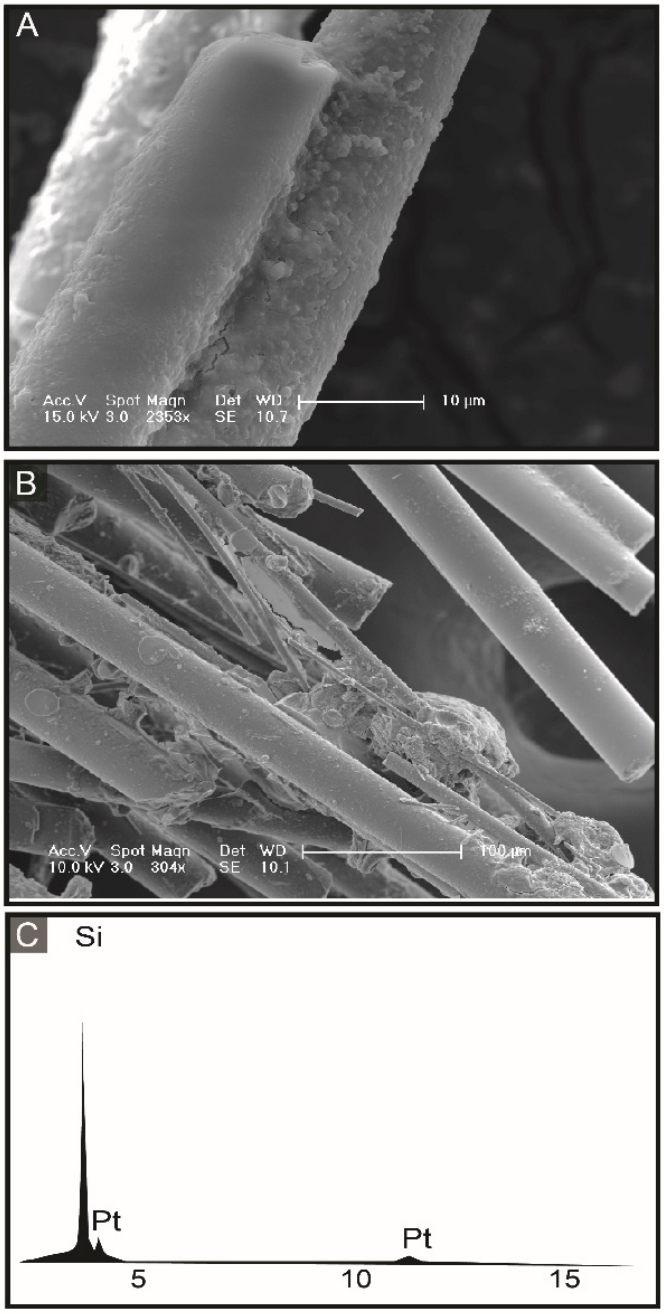

Figure S4. SEM images of pristine demosponge spicules in experiments after (A) 60 hours, and (B) 100 hours. (C) EDS spectra of panel B demonstrating the siliceous composition of the spicules. Pt peaks correspond to the coating.

REFERENCES CITED

Fein, J.B., Boily J.-F., Yee, N., Gorman-Lewis, D., Turner, B.F., 2005, Potentiometric titrations of *Bacillus subtilis* cells to low pH and a comparison of modeling approaches: Geochimica, et Cosmochimica, Acta, v. 69, p. 1123-1132, https://doi.org/10.1016/j.gca.2004.07.033.

Hao, W., Flynn, S.L., Kashiwabara, T., Alam, M.S., Bandara, S., Robbins, L.J., Alessi, D.S., Konhauser, K.O., 2019, The impact of ionic strength on the proton reactivity of clay minerals: Chemical Geology, v. 529, p. 1192-94, https://doi.org/10.1016/j.chemgeo.2019.119294.

Konhauser, K.O., 2009, Introduction to geomicrobiology, John Wiley & Sons, Chapter 3, p. 102.

Konhauser, K.O., Hao, W., Li, Y., von Gunten, K., Bishop, B.A., Alessi, D.S., Tarhan, L.G., O'Connell, B., Robbins, L.J., Planavsky, N.J. and Gingras, M.K., 2020, *Diopatra cuprea* worm burrow parchment: a cautionary tale of infaunal surface reactivity: Lethaia, https://doi.org/10.1111/let.12335.

Lalonde, S.V., Dafoe, L.T., Pemberton, S.G., Gingras, M.K., Konhauser, K.O., 2010, Investigating the geochemical impact of burrowing animals: Proton and cadmium adsorption onto the mucus lining of Terebellid polychaete worms: Chemical geology, v. 271, p. 44-51, https://doi.org/10.1016/j.chemgeo.2009.12.010

Liu, Y., Alessi, D.S., Owttrim, G.W., Petrash, D.A., Mloszewska, A.M., Lalonde, S.V., Martinez, R.E., Zhou, Q., Konhauser, K.O., 2015, Cell surface reactivity of Synechococcus sp. PCC 7002: Implications for metal sorption from seawater: Geochimica et Cosmochimica Acta, v., 169, p. 30-44, doi: https://doi.org/10.1016/j.gca.2015.07.033.

Newman, S.A., Mariotti, G., Pruss, S., & Bosak, T., 2016, Insights into cyanobacterial fossilization in Ediacaran siliciclastic environments: Geology, v. 44, p. 579–582, https://doi.org/0.1130 /G37791.1

Mullin J.B., Riley J.P., 1955, The colorimetric determination of silicate with special reference to sea and natural waters: Analytica Chimica Acta, v. 12, p. 162-176. https://doi.org/10.1016/S0003-2670(00)87825-3

Petrash, D.A., Lalonde, S.V., Gingras, M.K., Konhauser, K.O., 2011a, A surrogate approach to studying the chemical reactivity of burrow mucous linings in marine sediments: Palaios, v. 26, p. 594-600, https://doi.org/10.2110/palo.2010.p10-140r

Petrash, D.A., Lalonde, S.V., Raudsepp, M., Konhauser, K.O., 2011b, Assessing the importance of organic matrix materials in biofilm chemical reactivity: insights from proton and cadmium adsorption onto the commercially available biopolymer alginate: Geomicrobiology Journal, v. 28, p. 266-273.

Phoenix, V. R., Martinez, R.E., Konhauser, K.O., and Ferris, F.G., 2002, Characterization and Implications of the Cell Surface Reactivity of *Calothrix* sp. Strain KC97: Applied and environmental microbiology, v. 68, p. 4827–4834, https://doi.org/10.1128/AEM.68.10.4827–4834.2002.

Westall, J.C., 1982. FITEQL: A Computer Program for Determination of Chemical Equilibrium Constants from Experimental Data. Department of Chemistry, Oregon State University.